Sodium control in ultrathin $Cu(In,Ga)Se_2$ solar cells on transparent back contact for efficiencies beyond 12%

Yong Li[a], Guanchao Yin[b], Yao Gao[a], Tristan Köhler[a], Jan Lucaßen[a], Martina Schmid[a]*

[a]*Department of Physics, University of Duisburg-Essen & CENIDE, Lotharstraße 1, 47057 Duisburg, Germany*
[b]*School of Materials Science and Engineering, Wuhan University of Technology, Luoshi Road 122, 430070 Wuhan, China*

*Corresponding author. School of Materials Science and Engineering, Wuhan University of Technology, Luoshi Road 122, 430070 Wuhan, China.

E-mail address: guanchao.yin@whut.edu.cn (G. Yin)

Abstract: Ultrathin $Cu(In,Ga)Se_2$ (CIGSe) solar cells on transparent conductive oxide (TCO) back contacts combine advantages of ultrathin cells for reducing material consumption of rare indium and gallium and TCO-transparency benefited applications in tandems, bifacial configurations etc. However, their efficiencies are still limited and the back barrier potential is a primary reason from an electrical perspective. In this work, we explore the effects of Na doping by post deposition treatment (PDT) on the performance of ultrathin CIGSe solar cells on ITO ($Sn:In_2O_3$)-coated Na-free glass substrates. Na doping enhances not only the open circuit-voltage (V_{oc}) by increasing the doping level, but also the fill factor (FF) by switching the Schottky contact to an Ohmic contact at the CIGSe/ITO interface, which we propose is due to the increased recombination at the back interface. The optimum performance is achieved at a NaF dose of 2 mg with a top efficiency of 12.9%, which exhibits an enhancement by nearly 48% relative compared to the references without Na doping. To our best knowledge, this is the highest efficiency achieved for ultrathin cells (< 500 nm absorber thickness) on TCO without additional antireflection or back reflecting layer. Therefore, the results show that sodium control offers a solid basis for the development of ultrathin CIGSe cells on TCO in above-mentioned promising applications.

Keywords: semi-transparent, ultrathin $Cu(In,Ga)Se_2$ solar cells, post deposition treatment (PDT), sodium (Na) control, Schottky contact

1 Introduction

$Cu(In,Ga)Se_2$ (CIGSe) thin-film solar cells with sub-500 nm thick absorbers on transparent conductive oxides (TCOs), defined as semi-transparent ultrathin CIGSe solar cells, have been attracting intensive attention recently [1-6]. They combine advantages of ultrathin cells, which dramatically reduce the material consumption of

rare indium and gallium [1, 2], and TCO-transparency induced promising applications such as a top cells in tandem solar cells, bifacial configurations or solar windows [3, 6-8]. Previous investigations had been conducted for exploring these application possibilities mainly on Sn:In_2O_3 (ITO) due to its overall superior tradeoff between conductivity, transparency and thermal stability [7]. However, the performance of semi-transparent ultrathin CIGSe solar cells is strongly constraint with an efficiency lower than 10% [1-6], which is far below the one of their counterparts on Mo (15.2%) [9] and those with 2-3 μm absorber thickness (23.35%) [10]. Two primary challenges are responsible for this failure. One reason is the incomplete absorption due to the reduced absorber thickness. However, our previous work has experimentally demonstrated that semi-transparent ultrathin CIGSe solar cells are able to achieve absorption comparable to the one of their thick counterparts via well-designed light-trapping nanostructures [2]. Also, TCO back contacts allow ultrathin CIGSe solar cells to overcome the weakness of insufficient light absorption by applying them in tandem configurations as a top cell, as bifacial solar cells or in solar windows, where a certain transparency is mandatory [3, 8]. Another reason for the poor performance of semi-transparent ultrathin CIGSe solar cells is the inherent Schottky back contact resulting from a mismatch of work functions between TCO and CIGSe, which deteriorates the electrical properties in terms of blocking the hole transport [6, 8, 11].

It is well known that Na doping is crucial to increase the acceptor doping concentration in chalcopyrite absorbers via suppressing donor-like defects such as In_{Cu} and V_{se} and creating acceptor-like Na_{In} defects, thus improving the performance of CIGSe solar cells [12-14]. On the other hand, for cells on TCO, Na doping is able to catalyze the formation of interfacial GaO_x at the CIGSe/TCO interface by activating O atoms from TCO [15, 16]. GaO_x is highly resistive and n-typed in nature [7, 17]. It contributes to the formation of a reverse pn-junction at the back interface, thus blocking the hole transport and deteriorating the cell performance. Therefore, it will be quite likely that the influence of Na doping for semi-transparent ultrathin CIGSe solar cells differs from the case on Mo. A few previous studies addressed the investigation how the Na doping affects the formation of GaO_x and the performance of semi-transparent ultrathin CIGSe solar cells [3-6, 18]. However, the mechanism of the rear interface modification by GaO_x formation is not yet well understood and the reported experimental efficiencies still fail to go beyond 10%. Considering the promising advantages mentioned above, it will be highly meaningful to deepen the investigation of Na doping on the performance of semi-transparent ultrathin CIGSe solar cells and seek for higher efficiencies.

In this contribution, we applied a post deposition treatment (PDT) to introduce Na into ultrathin CIGSe absorbers on ITO-coated Na-free glass substrates and investigated how the Na doping influences the performance of semi-transparent ultrathin CIGSe solar cells. It is discovered that a proper amount of NaF doping is improving the open-circuit voltage (V_{oc}). More remarkably, Na introduction enables to remove the inherent Schottky contact and thus improves the fill factor (*FF*), which we propose is realized in terms of increasing the interface recombination at the CIGSe/ITO interface. Both effects contribute to the achievement of a best efficiency of 12.9% and an average of

12.1% at a NaF dose of 2 mg, which is relatively 48% higher compared to the cells without extra Na doping. The results show that semi-transparent ultrathin CIGSe solar cells can overcome their electrical drawbacks and thus lay a solid foundation for further applications, provided by proper light management.

2 Experiments

Barium-borosilicate glass 7059 (alkali content below 0.3%, purchased from CORNING) is selected to serve as alkali-free glass substrate. 300 nm thick ITO was produced in our laboratory by DC-sputtering onto the glass substrates at a rate of 2.0-2.5 Å/s. The native sheet resistance of ITO was identified as 15 Ω/sq directly and it dropped to below 10 Ω/sq after undergoing the heat treatment during the absorber fabrication.

CIGSe absorbers with sub-500 nm thickness were fabricated on top of ITO by 3-stage co-evaporation [19]. The substrate temperature in the 2nd stage was set to 450°C. On the one hand this low temperature facilitates the formation of a steep back Ga grading towards the back contact to reduce back recombination [19]. On the other hand it is likely to suppress the growth of GaO_x layers at the CIGSe/ITO interface [7]. Next, eight absorbers from one co-evaporation batch were equally divided into 4 groups, each of which underwent a post deposition treatment procedure with 0, 2, 4 and 8 mg of NaF powder, separately. We realized this by opening the PVD chamber and taking out all samples first and then putting back two samples for different amounts of Na doping whilst storing the others under vacuum. 15-minute PDT duration time and 360 °C substrate temperature were found as an optimum to ensure that all NaF powder was evaporated from the crucible in the Se atmosphere. For cell completion, a 50 nm thick layer of CdS was deposited by chemical-bath-deposition, followed by a 70 nm thick intrinsic ZnO (i-ZnO) and a 300 nm thick aluminum-doped (AZO) layer. Finally, Ni/Al finger front contacts were thermally evaporated on top of the samples and each sample was scribed into 8 sub-cells mechanically giving an active area of 0.5 cm^2.

X-ray fluorescence (XRF) was applied to characterize the absorber thickness (465 nm), Cu/(Ga+In) ratio (0.88) and Ga/(Ga+In) ratio (0.30). For performance evaluation, the current density-voltage (j-V) curves were measured under a standard AM 1.5 solar simulator as well as in dark condition at room temperature. During the measurements the samples were kept at a constant temperature of 25°C by being mounted onto a brass plate. To gain insight into the CIGSe/ITO interface, temperature dependent current density-voltage (jV-T) measurements were performed in the temperature range of 160-300 K. Capacitance-voltage (C-V) measurements were done under total dark environment at 100 kHz for evaluating the doping concentration of the absorbers. After the above-mentioned characterizations, the solar cells were damaged for carrying out glow discharge optical emission spectroscopy (GD-OES) to probe the Na, Cu, Ga, In depth profiles in the absorbers.

3 Results and Discussion

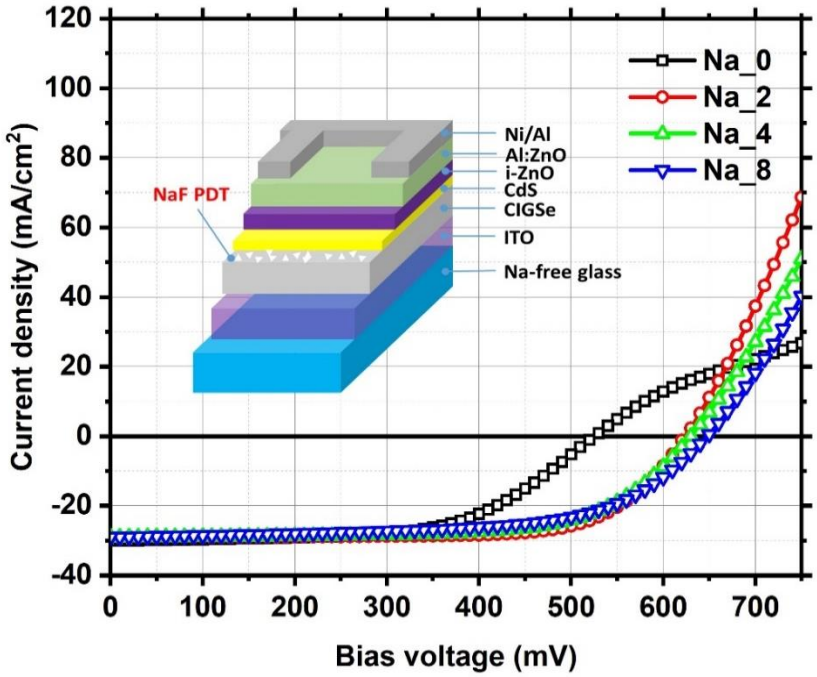

Figure 1. j-V curves of the best semi-transparent ultrathin CIGSe solar cells on ITO for different NaF PDT doses; the inset is the schematic illustration of a CIGSe solar cell on ITO

Table 1. Averaged j-V parameters (as well as the best cell's efficiency) and series resistance (R_s), net acceptor doping concentration (N_A), width of space charge region (d_{SCR}) of ultrathin cells on ITO with different NaF doping doses

name	PDT dose (mg)	V_{oc} (mV)	j_{sc} (mA/cm^2)	*FF* (%)	*Eff.* (%)	R_s (Ω/cm^2)	N_A (cm^{-3})	d_{SCR} (nm)	Best Eff. (%)
Na_0	0	513.6±7.3	29.1±0.6	55.1±3.0	8.2±0.7	17.4	3.18 * 10^{15}	498	9.3
Na_2	2	619.5±3.9	28.6±0.5	68.2±2.9	12.1±0.8	5.3	5.65 * 10^{15}	454	12.9
Na_4	4	624.1±6.2	28.4±0.6	64.9±2.6	11.5±0.6	7.3	6.35 * 10^{15}	447	12.1
Na_8	8	636.5±6.5	28.6±0.6	56.8±3.4	10.3±0.9	8.2	1.28 * 10^{16}	360	11.6

In **Figure 1**, the j-V curves of the best semi-transparent ultrathin solar cells on ITO with different NaF PDT doses are compared. It can be observed that the j-V curve without Na doping (denoted as Na_0) exhibits an S-shaped characteristic, where the current is heavily blocked in the forward bias. This phenomenon is commonly found for cells on TCO substrates and is attributed to the mismatch of work functions between CIGSe and TCO, which leads to a back barrier potential (Schottky contact) and gives rise to a competing space charge region opposed to the major CIGSe/CdS one [1-5, 18]. Interestingly, after Na doping, the S shaped behavior disappears completely and the Na-doped samples behave similarly to the ones on conventional Mo substrate with an

Ohmic back contact. This fact suggests that Na doping is likely to disable the Schottky contact at the rear interface of CIGSe/ITO and the detailed reasons will be discussed below.

To quantitatively evaluate the effects of Na doping on the performance of CIGSe solar cells, averaged j-V parameters are summarized in Table 1. Compared to the samples without Na doping (Na_0), 2-mg NaF dose (Na_2) enhances V_{oc} dramatically by more than 100 mV (from 513.6 to 619.5 mV). As the NaF dose increases further, V_{oc} continues to improve but only moderately to 624.1 mV for Na_4 and to 636.5 mV for Na_8. The maximum short-circuit current density (j_{sc}) of 29.1 mA/cm^2 is achieved for Na_0. Adding more NaF decreases j_{sc} slightly, but its value is relatively independent of the amount of the NaF dose and stays stable at around 28.5 mA/cm^2. As to the fill factor (FF), it improves from poor 55.1% for Na_0 to 68.2% for Na_2. Unlike the V_{oc}, further addition of NaF deteriorates FF. Consequently, efficiencies (Eff.) follow a similar trend as FF: it peaks at a value of 12.1% in average for Na_2, exhibiting a relative enhancement by 47.6% compared to Na_0. Actually, the best cell reaches an efficiency of 12.9% (as shown in Table 1), which is, to our best knowledge, the highest efficiency achieved so far for ultrathin CIGSe solar cells on TCO. It should be noted here that we also applied other Na doping paths (Na diffusing soda-lime glass and NaF precursor on ITO surface) for semi-transparent ultrathin CIGSe solar cells (not shown here) and they didn't exhibit the roll-over effect either (S-shaped characteristic in j-V curve). Despite full optimization of the NaF amount and substrate temperature, their performance is always inferior to the one using PDT doping. This could be related to the different Na introduction paths modifying the defects in the bulk [20-22] and/or at the back interface [4, 18] differently.

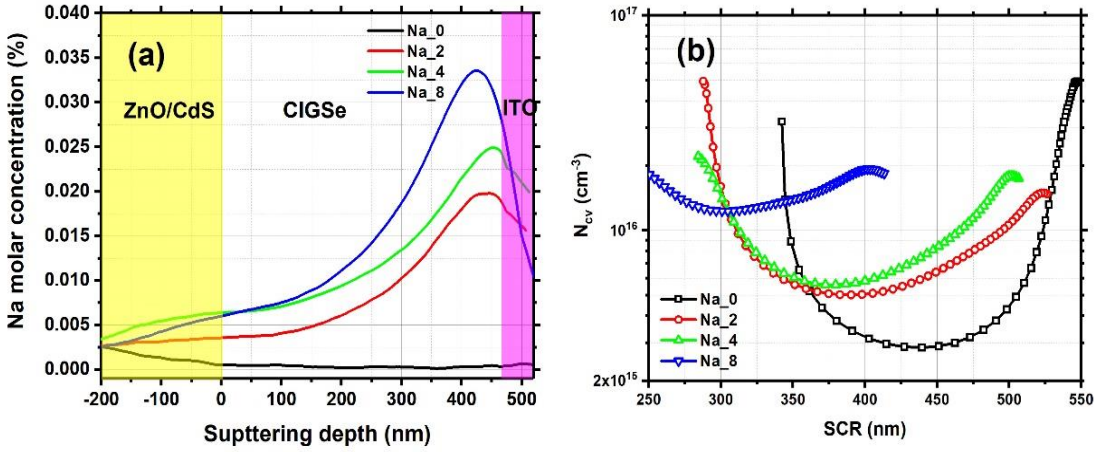

Figure 2. (a) Na concentration profiles measured by GD-OES and (b) net doping concentration depth profiles derived from C-V measurements for the absorbers with different NaF PDT doses

To better understand the changing trend of j-V parameters, we carried out GD-OES and C-V measurements to obtain the depth-resolved Na concentration and the doping

concentration (N_{cv}) profiles in the absorbers, respectively. As shown in **Figure 2**(a), Na_0 shows a significantly reduced Na concentration compared to the NaF doped samples. Absorbers with NaF doping show an increasing Na concentration towards the back CIGSe/ITO interface and this trend is more pronounced for a higher amount of NaF introduced. Figure. 2(b) reveals that as more NaF introduced, the fluctuation magnitude of N_{cv} across the whole absorber depth is gradually reduced. Simultaneously, N_{cv} becomes overall higher, which implies that Na is acting effectively to improve the acceptor doping level. For a more direct comparison, the acceptor concentration N_A was obtained via a Mott-Schottky plot [23] (shown in supporting information **Figure S1**), the width of the space charge region at zero bias deduced, and the results are summarized in Table 1. N_A is continuously increasing from $3.18*10^{15}$ cm^{-3} (Na_0) to $1.28*10^{16}$ cm^{-3} (Na_8), giving an increase of almost one order. Consequently, the width of the corresponding space charge region in the absorber decreases from 498 to 360 nm.

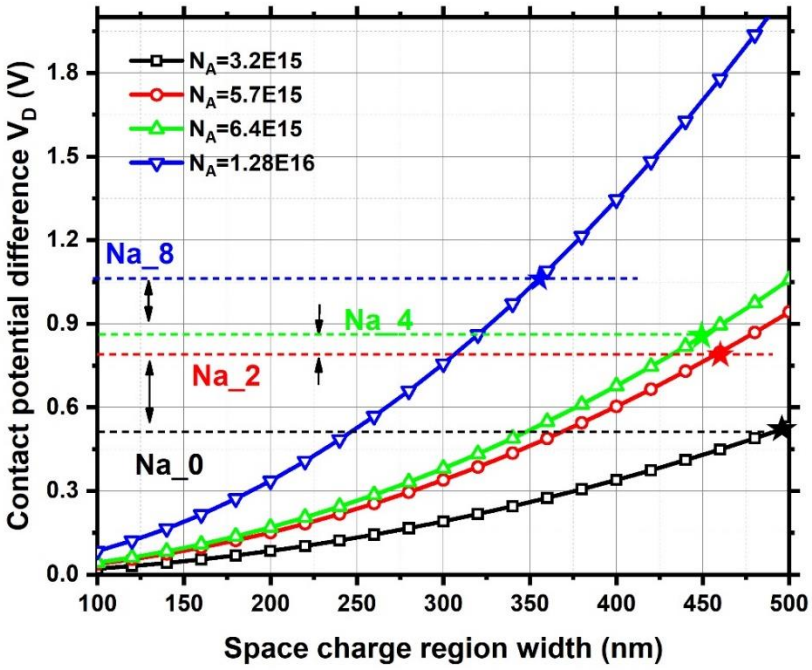

Figure 3. Dependence of contact potential difference (V_D) on SCR width (d_{SCR}) and experimental acceptor doping concentration (N_A); the corresponding V_D values for our experimental samples calculated by equation (1) are also marked (stars)

In order to fully understand the trade-off relation between N_A, SCR width (d_{SCR}) and V_{oc}, we may have a closer look at the theoretical relations. Since the contact potential difference (V_D) across a pn-junction is an indicator for V_{oc}, we can obtain the changing trend of V_{oc} from V_D. V_D is proposed to be a function of d_{SCR} and N_A according to the flowing equation for a single sided pn junction approximation [23]:

$$V_D = {d_{SCR}}^2 \frac{e}{2\varepsilon_r \varepsilon_0} \frac{N_A N_D}{N_A + N_D} \qquad (1)$$

Where e is the electron charge, N_D is the donor concentration of the n-type side (in our case, it is corresponding to the CdS/i-ZnO/AZO side), ε_r and ε_0 are the relative dielectric constant and vacuum dielectric constant, respectively. Setting N_D to a reasonable value

of $10*10^{15}$ cm^{-3} and ε_r to 13.6 (ε_0 = 1) [24], **Figure 3** shows the dependence of V_D on d_{SCR} calculated for various experimental N_A conditions. It can be simply concluded that a wide d_{SCR} together with a high N_A can guarantee a high V_D. A higher N_A typically induces a narrower d_{SCR}. Therefore, there exists a trade-off between N_A concentration and d_{SCR} for a maximum V_D. We also evaluated the corresponding contact potential difference V_D values by Mott-Schottky model (as shown in **Figure S1**), and they show a similar tendency as the single sided model.

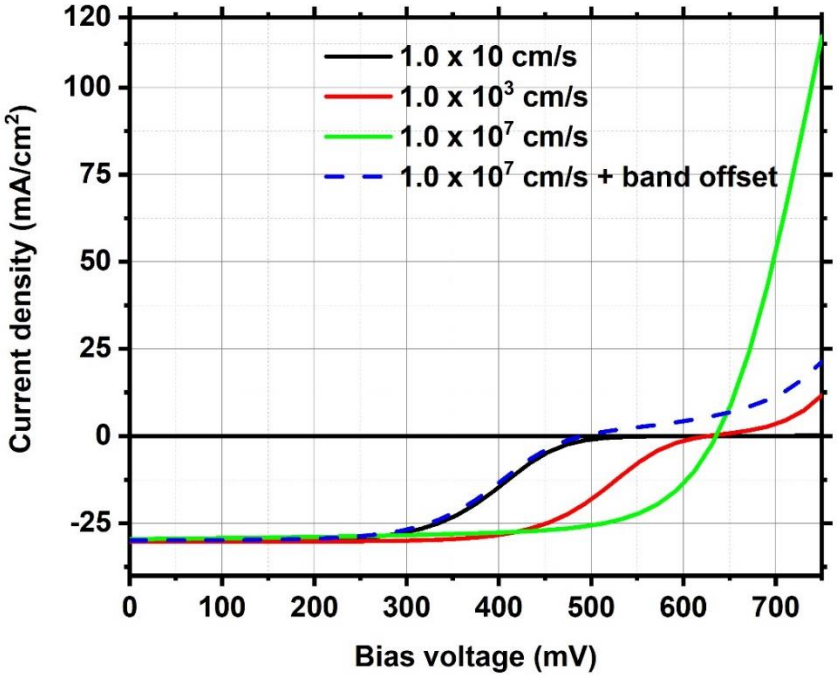

Figure 4. Dependence of simulated j-V curves of ultrathin CIGSe solar cells with a back potential of 0.4 eV on back interface recombination velocity and band offset

Coming back to the remaining question why the S-shaped characteristic of j-V curves disappears after Na doping, a similar phenomenon was also observed by Son et al. for Na-doped samples [18] and Chantana et al. for superstrate cells [25]. Since Na accumulation at the rear interface produces a high density of deep defects in the GaO_x layer as demonstrated by photoluminescence measurement, Son et al. assumed that it is the Na doping induced defects in the GaO_x layer facilitate the transport of holes in terms of tunneling and thus switch the Schottky contact to an Ohmic contact [18]. However, there was no solid evidence for this explanation. Chantana et al. introduced high density defects at the CIGSe/TCO interface by intentional modification of the TCO deposition parameters[25]. Since the TCO deposition was realized at room temperature the cells should be free of interfacial GaO_x and therefore tunneling-assisted hole transport is unlikely. Here, we propose a new mechanism for the explanation, namely an increased back recombination at the interface of CIGSe/ITO (resulting from the increased defect density by NaF PDT), which contributes to the disappearance of the S-shaped characteristic.

To verify this assumption, we performed SCAPS [26, 27] simulations for theoretical studies. A simple model is set up with an absorber thickness of 500 nm and an acceptor concentration of $4*10^{15}$ cm^{-3}[1]. A back barrier potential of 0.4 eV is fixed to create a Schottky contact. To make the model simple, only the recombination at the back interface is considered. More parameter information can be found in the supporting information **S2** and the definition file can be obtained from the authors. **Figure 4** represents the simulated j-V curves with a variation of back interface recombination velocity. We can observe, that for an interface recombination rate as low as 1*10 cm/s (solid dark line), the back barrier potential (Schottky contact) indeed leads to an S-shaped j-V curve. More remarkably, as the interface recombination velocity increases, the S-shaped characteristic is gradually abating and completely disappears when the back interface recombination reaches the order of $1*10^7$ cm/s. As stressed above, the underlying reason is the high back recombination velocity assisting the transport of holes, thus reducing the blocking effect due to the back barrier potential [28]. To further demonstrate it, we insert a 10 nm thick artificial CIGSe layer at the back interface between CIGSe and back contact with a 0.28 eV offset in the valence band to the 500 nm thick absorber. Notably, the S-shape characteristic (blue dotted line) reappears since the hole transport is hindered at the interface between the 10 nm thick artificial absorber and the 500 nm thick one. The obvious benefit of an increased back recombination velocity is the enhancement of the *FF*, which is in agreement with the conclusion that the Schottky contact can result in a drop of *FF* and thus a poor cell performance [27]. It should be emphasized here that the simulation results are contrary to the previous studies on Mo (Ohmic contact) where a reduced back recombination velocity is desirable [29]. It indicates that inserting a point-contact structure at the back interface may possibly do harm to semitransparent ultrathin CIGSe solar cells, which however will need further investigation.

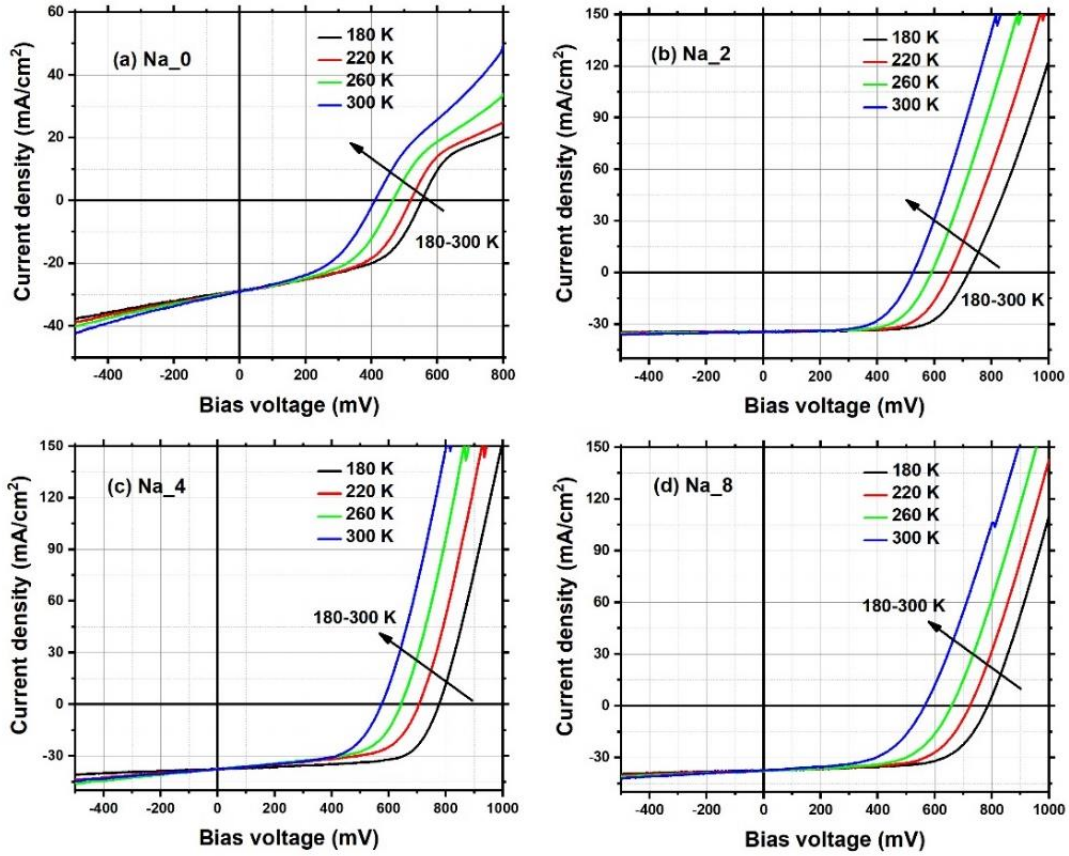

Figure 5. Temperature dependent j-VT curves taken under 1.3 suns for sample (a) Na_0, (b) Na_2, (c) Na_4, (d) Na_8

To further verify that Na doping reduces the barrier potential at the CIGSe/ITO interface, jV-T measurements were performed under an illumination intensity of around 1.3 sun in the temperature range of 160-300 K and representative j-V curves are shown in **Figure 5**. Due to the decrease of thermal energy of carriers against the back barrier potential, the S-shaped characteristic is reinforced as the temperature is dropping for Na_0. This poses a sharp contrast to Na doped samples where almost no obvious slope change in the forward bias is visible, which further implies that the effect of the barrier potential is reduced to a negligible level after Na doping.

In **Figure 6**, the dependence of V_{oc} on temperature is plotted for four samples. Via the following equation containing the activation energy of recombination (E_a), the barrier potential (Φ_b) can be estimated [30]:

$$V_{oc} = \frac{E_a}{e} - \frac{nkT}{e}\ln\left(\frac{J_{00}}{Jsc}\right) \quad (2)$$

Where k is the Boltzmann constant, n is the diode ideality factor, and j_{sc} and j_{00} denote the short-circuit current density and the prefactor of saturation current density, respectively. E_a is typically equal to the minimum bandgap (E_g) of CIGSe for an Ohmic contact and is modified to $E_g - \Phi_b$ when the back barrier potential is not negligible

[31]. Based on the equation, E_a can be extrapolated from the linear regime in V_{oc} (T) curves [30]. E_a is deduced to be 0.75 eV for Na_0, and is increased largely to 1.0 eV for Na_2. Further doping continues to enhance E_a by decreasing Φ_b but in a moderate magnitude. E_a reaches around 1.1 eV for Na_8 and is almost equal to the minimum E_g (1.12 eV calculated from GD-OES measured Ga/(Ga+In) ratio, shown in the supporting information **Figure S3**). Therefore, we can deduce that the barrier potential Φ_b is 0.37 eV for Na_0 and the Na doping reduces the barrier potential to less than 0.2 eV, which can be treated as Ohmic contact [32]. This is why the S-shaped characteristic is not observed in the Na doped cells. In the previous studies, it has been reported that inserting a hole transport layer [4, 6] or implementing effective light trapping structures at the CIGSe/ITO interface [2] are effective methods to reduce the back barrier potential. Here, we demonstrate the third approach, namely Na doping.

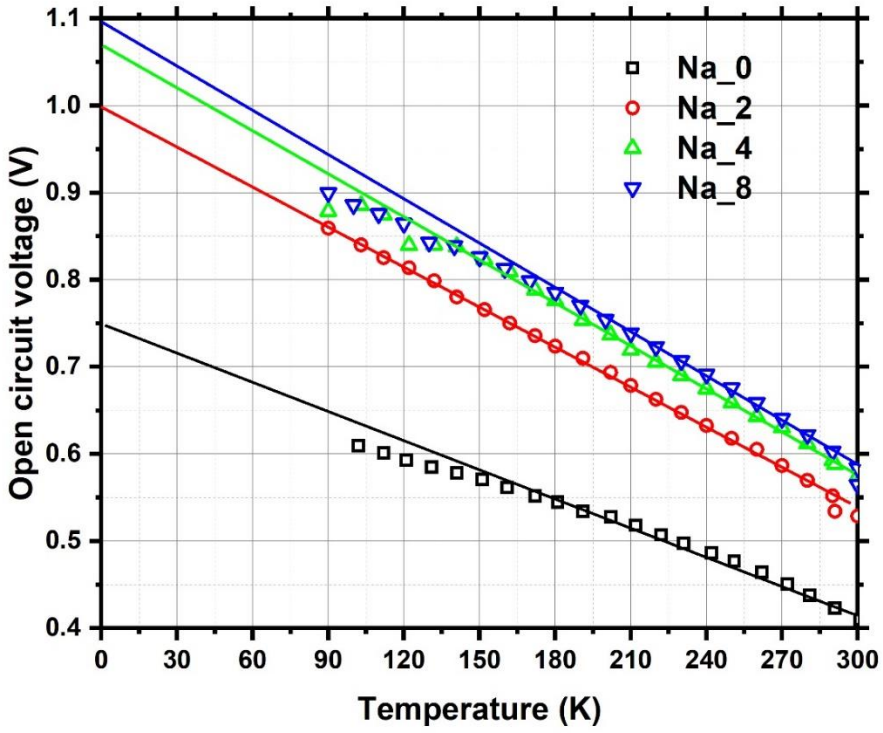

Figure 6. Dependence of V_{oc} on cell temperature

A divergence between experiments and simulations is the changing dependence of *FF* on recombination velocity. *FF* starts to decrease experimentally while it is continuously rising in the simulations as the Na dose further increases. To interpret it, experimental values of series resistance (R_s) are deduced by the derivative of experimental j-V curves at zero bias voltage and are also compared in Table 1. We can observe the increase of R_s as Na doping increases, which is the reason for the experimental drop in *FF*. Na-induced GaO_x growth is assumed to be responsible for the increase of R_s. As reported in Ref.[18], GaO_x is a highly resistive material and the existence of Na can catalyze the

growth of GaO_x. More Na incorporation indicates a thicker GaO_x layer, and leads to an increase of R_s and thus deteriorates the *FF* of the experimental cells, which is however not considered in the simulations. As to the slight drop in the experimental j_{sc} after the introduction of Na, this is linked to the change of d_{SCR}. Na_0 has the widest d_{SCR} with a value of 498 nm, hence penetrating the entire absorber thickness (465 nm), which can ensure an optimum collection of photo-generated carriers at zero bias. With the increase of Na doping, d_{SCR} is less than the absorber thickness and therefore leads to certain recombination at the rear interface of CIGSe/ITO. However, since the net value of electron diffusion length (the estimated value is around 300 nm for our samples) plus d_{SCR} is always larger than the absorber thickness, the collection of photo-generated carriers is only slightly dependent on the back recombination at zero bias. This is why j_{sc} drops slightly and remains almost stable after Na doping.

4 Conclusions

In this work, we investigated the effects of Na doping on the performance of semi-transparent ultrathin CIGSe solar cells on ITO. Apart from the pronounced increase of acceptor concentration and resulting enhancement of V_{oc}, Na doping is also capable of improving *FF* via eliminating the Schottky contact at the rear interface of CIGSe/ITO. We propose and demonstrate that it is the high recombination velocity at the rear interface that assists the transport of holes and thus switches the Schottky contact to an Ohmic contact. Consequently, under optimized conditions of 2 mg NaF-doping a maximum efficiency of 12.9% is achieved, which is, up to now, the highest efficiency obtained for semi-transparent ultrathin CIGSe solar cells.
Finally, we stress here, that semi-transparent CIGSe solar cells offer many application possibilities where partial transparency is required. However, the applications are not developed well due to poor base efficiencies. In this work, the demonstration of the removal of Schottky contact on ITO via simple Na doping and achievement of high base efficiencies pave the path for those promising applications.

5 Acknowledgement

All authors would like to express their sincere gratitude to Klaus Pärschke for technical support, and to Reiner Klenk for the discussions. The XRF and GD-OES measurements were performed on an instrument funded by the Deutsche Forschungsgemeinschaft (DFG, German Research Foundation) – INST 20876/324-1 FUGG and are acknowledged as follows: “Gefördert durch die Deutsche Forschungsgemeinschaft (DFG) – Projektnummer INST 20876/324-1 FUGG”. Y. Li specially acknowledges the financial support of Chinese Scholarship Committee, and G. Yin the funding from National Natural Science Foundation of China (NSFC, 51802240) and the funding support of the Fundamental Research Funds for the Central Universities (WUT:183101002, 193201003).

6 References

[1] G. Yin, M. Song, M. Schmid, Rear point contact structures for performance enhancement of semi-transparent ultrathin Cu(In,Ga)Se2 solar cells, Sol. Energy Mater. Sol. Cells, 195 (2019) 318-322.

[2] G. Yin, M.W. Knight, M.-C. van Lare, M.M. Solà Garcia, A. Polman, M. Schmid, Optoelectronic Enhancement of Ultrathin CuIn1-xGaxSe2Solar Cells by Nanophotonic Contacts, Adv. Opt. Mater., 5 (2017) 1600637.

[3] D. Kim, S.S. Shin, S.M. Lee, J.S. Cho, J.H. Yun, H.S. Lee, J.H. Park, Flexible and Semi‐Transparent Ultra‐Thin CIGSe Solar Cells Prepared on Ultra‐Thin Glass Substrate: A Key to Flexible Bifacial Photovoltaic Applications, Adv. Funct. Mater., (2020) 2001775.

[4] M. Saifullah, S. Rasool, S. Ahn, K. Kim, J.S. Cho, J.S. Yoo, W.S. Shin, J.H. Yun, J.H. Park, Performance and Uniformity Improvement in Ultrathin Cu(In,Ga)Se2 Solar Cells with a WOx Nano-Interlayer at the Absorber/Transparent Back-Contact Interface, ACS Appl Mater Interfaces, (2019) 655-665.

[5] M. Saifullah, D. Kim, J.-S. Cho, S. Ahn, S. Ahn, J.H. Yun, H.S. Lee, J.H. Park, The role of NaF post-deposition treatment on the photovoltaic characteristics of semitransparent ultrathin Cu(In,Ga)Se2 solar cells prepared on indium-tin-oxide back contacts: a comparative study, J. Mater. Chem. A, 7 (2019) 21843-21853.

[6] J.K. Larsen, H. Simchi, P. Xin, K. Kim, W.N. Shafarman, Backwall superstrate configuration for ultrathin Cu(In,Ga)Se2 solar cells, Appl. Phys. Lett., 104 (2014) 033901.

[7] T. Nakada, Y. Hirabayashi, T. Tokado, D. Ohmori, T. Mise, Novel device structure for Cu(In,Ga)Se2 thin film solar cells using transparent conducting oxide back and front contacts, Sol. Energy, 77 (2004) 739-747.

[8] H. Simchi, J. Larsen, K. Kim, W. Shafarman, Improved Performance of Ultrathin Cu(InGa)Se2 Solar Cells With a Backwall Superstrate Configuration, IEEE J. Photovoltaics, 4 (2014) 1630-1635.

[9] L.M. Mansfield, A. Kanevce, S.P. Harvey, K. Bowers, C. Beall, S. Glynn, I.L. Repins, Efficiency increased to 15.2% for ultra-thin Cu(In,Ga)Se2 solar cells, Prog. Photovoltaics Res. Appl., (2018) 1-6.

[10] M. Nakamura, K. Yamaguchi, Y. Kimoto, Y. Yasaki, T. Kato, H. Sugimoto, Cd-Free Cu(In,Ga)(Se,S)2 Thin-Film Solar Cell With Record Efficiency of 23.35%, IEEE J. Photovoltaics, 9 (2019) 1863-1867.

[11] H. Simchi, B.E. McCandless, T. Meng, W.N. Shafarman, Structure and interface chemistry of MoO3 back contacts in Cu(In,Ga)Se2 thin film solar cells, J. Appl. Phys., 115 (2014) 033514.

[12] S.-H. Wei, S.B. Zhang, A. Zunger, Effects of Na on the electrical and structural properties of CuInSe2, J. Appl. Phys., 85 (1999) 7214-7218.

[13] D. Rudmann, A.F. da Cunha, M. Kaelin, F. Kurdesau, H. Zogg, A.N. Tiwari, G. Bilger, Efficiency enhancement of Cu(In,Ga)Se2 solar cells due to post-deposition Na incorporation, Appl. Phys. Lett., 84 (2004) 1129-1131.

[14] J. Ramanujam, U.P. Singh, Copper indium gallium selenide based solar cells – a review, Energy Environ. Sci., 10 (2017) 1306-1319.
[15] M.D. Heinemann, V. Efimova, R. Klenk, B. Hoepfner, M. Wollgarten, T. Unold, H.-W. Schock, C.A. Kaufmann, Cu(In,Ga)Se2 superstrate solar cells: prospects and limitations, Prog. Photovoltaics Res. Appl., 23 (2015) 1228-1237.
[16] L. Kronik, D. Cahen, H.W. Schock, Effects of Sodium on Polycrystalline Cu(In,Ga)Se2 and Its Solar Cell Performance, Adv. Mater., 10 (1998) 31-36.
[17] T. Nakada, Microstructural and diffusion properties of CIGS thin film solar cells fabricated using transparent conducting oxide back contacts, Thin Solid Films, 480-481 (2005) 419-425.
[18] Y.-S. Son, H. Yu, J.-K. Park, W.M. Kim, S.-Y. Ahn, W. Choi, D. Kim, J.-h. Jeong, Control of Structural and Electrical Properties of Indium Tin Oxide (ITO)/Cu(In,Ga)Se2 Interface for Transparent Back-Contact Applications, J. Phys. Chem. C, 123 (2019) 1635-1644.
[19] G. Yin, V. Brackmann, V. Hoffmann, M. Schmid, Enhanced performance of ultra-thin Cu(In,Ga)Se 2 solar cells deposited at low process temperature, Sol. Energy Mater. Sol. Cells, 132 (2015) 142-147.
[20] H. Stange, S. Brunken, H. Hempel, H. Rodriguez-Alvarez, N. Schäfer, D. Greiner, A. Scheu, J. Lauche, C.A. Kaufmann, T. Unold, D. Abou-Ras, R. Mainz, Effect of Na presence during CuInSe2 growth on stacking fault annihilation and electronic properties, Appl. Phys. Lett., 107 (2015).
[21] R. Mainz, E. Simsek Sanli, H. Stange, D. Azulay, S. Brunken, D. Greiner, S. Hajaj, M.D. Heinemann, C.A. Kaufmann, M. Klaus, Q.M. Ramasse, H. Rodriguez-Alvarez, A. Weber, I. Balberg, O. Millo, P.A. van Aken, D. Abou-Ras, Annihilation of structural defects in chalcogenide absorber films for high-efficiency solar cells, Energy Environ. Sci., 9 (2016) 1818-1827.
[22] N. Zakay, H. Stange, H. Alpern, D. Greiner, D. Abou-Ras, R. Mainz, I. Balberg, O. Millo, D. Azulay, Phototransport Properties of CuInSe2 Thin Films: The Influence of Na and Planar Defects, Physical Review Applied, 14 (2020).
[23] S.M. Sze, K.K. Ng, Physics of semiconductor devices, John Wiley & Sons, Hoboken, New Jersey. Published simutaneously in Canada., 2007.
[24] R. Kotipalli, O. Poncelet, G. Li, Y. Zeng, L.A. Francis, B. Vermang, D. Flandre, Addressing the impact of rear surface passivation mechanisms on ultra-thin Cu(In,Ga)Se 2 solar cell performances using SCAPS 1-D model, Sol. Energy, 157 (2017) 603-613.
[25] J. Chantana, H. Arai, T. Minemoto, Trap-assisted recombination for ohmic-like contact at p-type Cu(In,Ga)Se2/back n-type TCO interface in superstrate-type solar cell, J. Appl. Phys., 120 (2016) 045302.
[26] M. Burgelman, P. Nollet, S. Degrave, Modelling polycrystalline semiconductor solar cells, Thin Solid Films, 361-362 (2000) 527-532.
[27] Q. Cao, O. Gunawan, M. Copel, K.B. Reuter, S.J. Chey, V.R. Deline, D.B. Mitzi, Defects in Cu(In,Ga)Se2 Chalcopyrite Semiconductors: A Comparative Study of Material Properties, Defect States, and Photovoltaic Performance, Adv. Energy Mater., 1 (2011) 845-853.

[28] S. Rebecca, S-Shaped Current–Voltage Characteristics in Solar Cells: A Review, IEEE J. Photovoltaics, 9 (2019) 1477-1484.
[29] B. Vermang, V. Fjällström, J. Pettersson, P. Salomé, M. Edoff, Development of rear surface passivated Cu(In,Ga)Se2 thin film solar cells with nano-sized local rear point contacts, Sol. Energy Mater. Sol. Cells, 117 (2013) 505-511.
[30] S.S. Hegedus, W.N. Shafarman, Thin-film solar cells: device measurements and analysis, Prog. Photovoltaics Res. Appl., 12 (2004) 155-176.
[31] T. Ott, F. Schönberger, T. Walter, D. Hariskos, O. Kiowski, O. Salomon, R. Schäffler, Verification of phototransistor model for Cu(In,Ga)Se 2 solar cells, Thin Solid Films, 582 (2015) 392-396.
[32] R. Scheer, H.-W. Schock, Chalcogenide Photovoltaics Physics, Technologies, and Thin Film Devices, WILEY-VCH Verlag & Co. KGaA, Boschstr. 12, 69469 Weinheim, Germany, 2011.